

**Spontaneous atomic shuffle in flat terraces: Ag(100)**F. Montalenti,<sup>1,2,\*</sup> A. F. Voter,<sup>2</sup> and R. Ferrando<sup>3</sup><sup>1</sup>*INFN, Dipartimento di Scienza dei Materiali, Università di Milano-Bicocca, Via Cozzi 53, 20125 Milano, Italy*<sup>2</sup>*Theoretical Division, Los Alamos National Laboratory, Los Alamos, New Mexico, 87545*<sup>3</sup>*INFN and CFSBT/CNR, Dipartimento di Fisica dell'Università di Genova, via Dodecaneso 33, 16146 Genova, Italy*

(Received 9 April 2002; revised manuscript received 5 July 2002; published 11 November 2002)

We study the temporal evolution of a flat Ag(100) surface in the temperature range 300–600 K. Using a recent version of the temperature-accelerated dynamics method, we are able to simulate very long time scales, ranging from milliseconds at 600 K to several months at 300 K. Interesting diffusion mechanisms are observed. In particular, the spontaneous creation of short-lived adatom–vacancy pairs leads to diffusion of the surface atoms within the surface.

DOI: 10.1103/PhysRevB.66.205404

PACS number(s): 68.35.Fx, 66.30.Fq, 82.20.Db

**I. INTRODUCTION**

Crystal growth, catalysis, and chemical reactions at surfaces are among the most popular research subjects in the present surface science community. Such processes are of formidable complexity, so that theoretical modeling, experimental techniques, and data interpretation are in constant development. One final goal is to reach a microscopic understanding of these phenomena, possibly starting from the basic constituents of solid surfaces: the atoms. Clearly, the knowledge of diffusion mechanisms and rates for isolated adatoms, clusters, or islands is a key step in attempting to model more complex processes. Recent results have shown that, even for simple metal systems, the present knowledge of the actual diffusion paths and energetics is far from complete, so that realistic simulations are still needed. Indeed, newly discovered diffusion mechanisms are continuously introduced. A few examples are given in Ref. 1. Three independent studies reported within the last two years have shown the importance of the role of surface<sup>2,3</sup> and bulk<sup>4</sup> vacancies, naturally present in real solids at equilibrium, in determining mobility at surfaces.

In this paper we show, using temperature-accelerated dynamics (TAD)<sup>5–7</sup> simulations, that even starting from an ideal, vacancy-free Ag(100) surface, the spontaneous creation of short-lived vacancies leads to appreciable diffusion of the surface atoms within the surface, at temperatures well below the melting point. The present results, together with those reported in Refs. 2,3, show that metal surfaces are much more dynamic than previously realized. Recalling that the typical scanning tunneling microscope (STM) temporal resolution is of the order of  $\sim 1$  s, our results show that, even well below the melting point, surface atoms on flat terraces are very likely to switch position between subsequent STM images. We note that this motion could influence diffusion of adatoms or islands on the surface itself.

Exploiting the boost in the dynamics given by the TAD method<sup>5</sup> in its most recent version,<sup>6</sup> we are able to simulate time scales ranging from ms at  $T=600$  K, to several months at  $T=300$  K, with full atomistic detail. As demonstrated by the results reported in Sec. III C, reaching these long time scales is crucial in order to unravel the complex dynamics of the system.

**II. THE TAD METHOD****A. Original formulation**

We recall that the TAD method<sup>5</sup> requires the harmonic approximation to the transition state theory (hTST) to hold, so that the rate  $k_i$  of a diffusion mechanism  $i$  with activation energy  $E_i$  and frequency prefactor  $\nu_{0,i}$  is described by the Arrhenius law

$$k_i = \nu_{0,i} \exp(-E_i/k_B T), \quad (1)$$

where  $T$  is the substrate temperature and  $k_B$  the Boltzmann constant. The TAD method allows one to simulate the long time required for a system to escape from a state  $A$  at a low temperature  $T_{\text{low}}$  by exploiting the faster dynamics at a higher temperature  $T_{\text{high}}$ . This is done by collecting a sequence of escape times  $t_{i,\text{high}}$  from  $A$  at  $T_{\text{high}}$ , and by extrapolating each of them to low temperature using the simple formula

$$t_{i,\text{low}} = t_{i,\text{high}} e^{E_i(\beta_{\text{low}} - \beta_{\text{high}})}, \quad (2)$$

where  $\beta_{\text{low}} = 1/(k_B T_{\text{low}})$  and  $\beta_{\text{high}} = 1/(k_B T_{\text{high}})$ . The event with the shortest time  $t_{\text{low,short}}$ , among the sequence of extrapolated times at  $T_{\text{low}}$ , is the event that the system chooses to escape from the state at  $T_{\text{low}}$ . Introducing an assumed lower bound  $\nu_{\text{min}}$  for the frequency prefactor, together with an uncertainty level  $\delta$ , it is possible to demonstrate<sup>5</sup> that after a total simulation time

$$t_{\text{high,stop}}^{\text{TAD}} \equiv \frac{\ln(1/\delta)}{\nu_{\text{min}}} \left( \frac{\nu_{\text{min}} t_{\text{low,short}}}{\ln(1/\delta)} \right)^{\beta_{\text{high}}/\beta_{\text{low}}} \quad (3)$$

is reached at  $T_{\text{high}}$ ,  $t_{\text{low,short}}$  can be declared, with uncertainty  $\delta$ , to be the shortest extrapolated time for escape from state  $A$  (for example,  $\delta=0.05$  means that we are at least 95% confident that the event with the shortest possible extrapolated time has been determined). At this point the event can be accepted; i.e., the system is moved out of  $A$  through the mechanism that generated  $t_{\text{low,short}}$ , the simulation clock is advanced by  $t_{\text{low,short}}$  and the whole procedure is begun again in the new state.

This procedure can be represented graphically by plotting the logarithm of inverse time versus  $\beta$ , as shown in Fig. 1. The progression of the high-temperature trajectory corre-

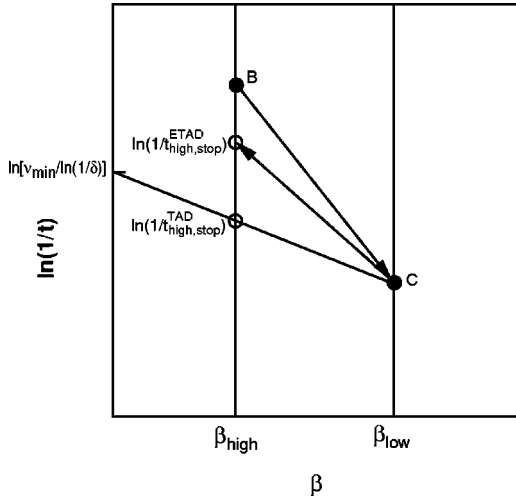


FIG. 1. Graphical representation of the TAD method, showing the logarithm of inverse time versus inverse temperature. Time propagates downward along the vertical lines. Attempted events observed during the high-temperature trajectory (e.g., point B) are extrapolated along a line with slope equal to the negative of the activation barrier to obtain the time at low temperature (point C). In the original TAD method, the high-temperature trajectory is terminated at the intersection with the “stop” line, indicated by  $t_{\text{high,stop}}^{\text{TAD}}$ . If the minimum barrier for escape from this state is known, the trajectory can be terminated sooner, at  $t_{\text{high,stop}}^{\text{ETAD}}$ , obtained by extrapolating back up from the low temperature to the high temperature along a line with a slope equal to the negative of this minimum barrier.

sponds to (nonlinear) motion downward along the vertical time line at  $\beta = \beta_{\text{high}}$ . If an event occurs at point B, its corresponding time at  $T_{\text{low}}$  (point C) is simply found by extrapolating along a line with slope equal to the negative of its barrier height. Although typically a few other events will occur before the trajectory is stopped, for simplicity here we only display the extrapolation for the event that has the shortest time at  $T_{\text{low}}$ . To find the stop time, we construct a line (the stop line) connecting  $\nu_{\text{min}}/\ln(1/\delta)$  on the y axis with the current shortest-time event on the low-temperature time line (point C). The intersection of this stop line with the high-temperature time line defines the stop time  $t_{\text{high,stop}}^{\text{TAD}}$ , which we can understand in the following way. Imagine that the trajectory is run a bit beyond the stop time and a new event occurs. We compare  $\Delta E$ , the barrier for the new event, to  $S$ , the negative of the slope of the stop line. If  $\Delta E \geq S$ , the new event does not replace the candidate event (at point C), because it extrapolates to a longer time at low temperature. If  $\Delta E < S$ , it could extrapolate to a shorter time, but, having specified the minimum prefactor  $\nu_{\text{min}}$ , we can rule out this possibility with certainty  $1 - \delta$ . This is because for any line passing through  $\nu_{\text{min}}/\ln(1/\delta)$ , the intersection of that line with a vertical time line corresponds to the time (at that temperature) for which a pathway with prefactor  $\nu_{\text{min}}$  and barrier  $S$  will have revealed itself (through an attempted escape) with probability  $1 - \delta$ . For barriers lower than  $S$ , the certainty is even greater that such a pathway is not hiding. A pathway with a prefactor lower than  $\nu_{\text{min}}$  could still be hid-

den, but we have assumed that no such pathways exist. Thus, terminating the trajectory at  $t_{\text{high,stop}}$ , allows us to say with a certainty of at least  $1 - \delta$  that the correct event is being accepted.

### B. Further boost for the TAD method

A method to further accelerate the dynamics within the TAD scheme was proposed very recently.<sup>6</sup> It was shown that, if the lowest activation energy  $E_{\text{min}}$  to escape out of a state is known, the total simulation time needed before accepting a transition can be computed using

$$t_{\text{high,stop}}^{\text{ETAD}} = t_{i,\text{high}} \exp[(E_i - E_{\text{min}})(\beta_{\text{low}} - \beta_{\text{high}})], \quad (4)$$

instead of Eq. (3), allowing one to shorten the simulation time significantly. Referring again to Fig. 1, the justification of this ETAD (the letter E in the acronym ETAD reminds us that the minimum barrier is known) procedure is easily seen. After the event at point B is observed, leading to the extrapolated time at point C,  $t_{\text{high,stop}}^{\text{ETAD}}$  is obtained from Eq. (4) by extrapolating from  $T_{\text{low}}$  back to  $T_{\text{high}}$  along a line with slope  $-E_{\text{min}}$ . Any event occurring after this time can only extrapolate to a shorter time at  $T_{\text{low}}$  if it has a barrier lower than  $E_{\text{min}}$ , which it cannot if  $E_{\text{min}}$  is indeed the lowest barrier for escape from this state.

In the common case where the first escape from the state corresponds to an event with activation energy  $E = E_{\text{min}}$ , from Eq. (4), one obtains  $t_{\text{high,stop}}^{\text{ETAD}} = t_{\text{high}}$ : the event is accepted as soon as it is detected. If the value of  $E_{\text{min}}$  is known exactly, this new procedure is exact: no new approximations beyond the ones in the original TAD method are required. In general,  $E_{\text{min}}$  can be determined by taking into account the total time  $\tau$  spent in all the visits to this state since the beginning of the simulation. The lowest barrier observed so far during this time can be declared the official lowest barrier  $E_{\text{min}}$  for escape from this state (with uncertainty  $\delta$ ) when  $\tau$  exceeds  $\tau_{\text{min}}$ , given by

$$\tau_{\text{min}} = \frac{\ln(1/\delta)}{\nu_{\text{min}}} \exp(E_{\text{min}}\beta_{\text{high}}). \quad (5)$$

This follows from an argument analogous to that given above for the TAD stop line; an event with prefactor  $\nu_{\text{min}}$  and a barrier less than  $E_{\text{min}}$  has a probability less than  $\delta$  of still being hidden after time  $\tau_{\text{min}}$  is reached. This procedure thus guarantees, within the uncertainty  $\delta$  of the TAD simulation, that  $E_{\text{min}}$  is found exactly. Reaching the simulation time  $\tau_{\text{min}}$  typically requires several visits to the state.<sup>6</sup> Some additional boost is obtained in successive revisits before  $\tau_{\text{min}}$  is achieved, as discussed in Ref. 6, but it is not very significant for systems that seldom revisit the same state (although there is the possibility of supplying  $E_{\text{min}}$  externally, also discussed in Ref. 6). In the present case, however, we can exploit the fact that the system spends most of its time in (and continually revisits) the flat-surface state. We discuss this below.

## III. SIMULATIONS

### A. Parameters

We now describe the results of the TAD simulations and the way we exploited the minimum-barrier concept for the

particular system investigated in this work. We studied the long-time behavior of an ideal Ag(100) surface at four different temperatures: 300, 400, 500, and 600 K. The simulation slab consisted of 6 layers of Ag atoms, with each layer composed of 98 atoms. The three bottom layers were kept frozen. Periodic boundary conditions were applied in the surface plane, and the lattice constant was determined by taking into account thermal expansion. The interatomic interaction was described by an embedded-atom method (EAM)<sup>8</sup> potential.<sup>9</sup> Although no surface data were included in the fit, this potential gives a very good prediction of the adatom diffusion barriers both from first principles<sup>10</sup> and experiments.<sup>11</sup> The temperature was controlled using a Langevin thermostat with a friction term set to  $10^{12} \text{ s}^{-1}$ .

Concerning the TAD parameters, we chose to work with an uncertainty of  $\delta=0.05$ , and we set the minimum prefactor  $\nu_{\min}$  to  $2 \times 10^{12} \text{ s}^{-1}$ . This choice was based on a set of prefactor calculations (we used the Vineyard expression of Ref. 12) preceding the actual simulations. To confirm that the value of  $\nu_{\min}$  was appropriate, after the TAD simulations were run, we checked the frequency prefactors for a large number of diffusion mechanisms detected during the simulations; all were indeed higher than  $\nu_{\min}$ . To accelerate the dynamics, we set  $T_{\text{high}}=1000 \text{ K}$  in the most ordered state (flat surface), where all activation energies are very high so that more boost is needed, while we reduced  $T_{\text{high}}$  by 30% in all the other configurations (for a discussion of the criteria used to choose  $T_{\text{high}}$ , see Refs. 5,13). A critical study of possible anharmonic effects is reported in Sec. III F.

### B. Boost in the dynamics

At each temperature, we ran TAD simulations until  $\sim 1000$  transitions were detected, giving simulation times of  $\sim 0.5 \text{ ms}$ ,  $\sim 0.1 \text{ s}$ ,  $\sim 3.5 \text{ min}$ , and  $\sim 2.4 \text{ yr}$  at 600, 500, 400, and 300 K, respectively. To reach these extremely long time scales, it was crucial to reduce the CPU time, by exploiting Eq. (4) instead of Eq. (3). As we already emphasized in Sec. II B, this is possible when information on the minimum barrier  $E_{\min}$  to escape from a state is available. We recall that the experimental melting temperature for Ag is  $T_m=1234 \text{ K}$ , so that  $T \leq T_m/2$  in the whole  $T$  range considered here. As a consequence, it was easy for us to guess in advance that the system would spend most of its time in the ordered state characterized by a perfectly flat surface.<sup>14</sup> So, before running the TAD simulations, we investigated possible escape paths out of this state by using short-time (few ns) MD simulations at  $T=1000 \text{ K}$ , and computing the activation energies of the detected mechanisms using the nudged elastic band method.<sup>15</sup> In this preliminary study, we found that the diffusion mechanism with the lowest activation barrier was the Frenkel-pair formation (see Sec. III C for a detailed description), with an activation energy of  $E=1.3 \text{ eV}$ .<sup>16</sup> We then supplied to the TAD code this  $E_{\min}$  barrier for the flat-surface state, and we instructed the code to use Eq. (4) instead of Eq. (3) each time the system was in this state. For all the other configurations visited by the system during its evolution, we did not supply any *a priori* information on the dynamics, and

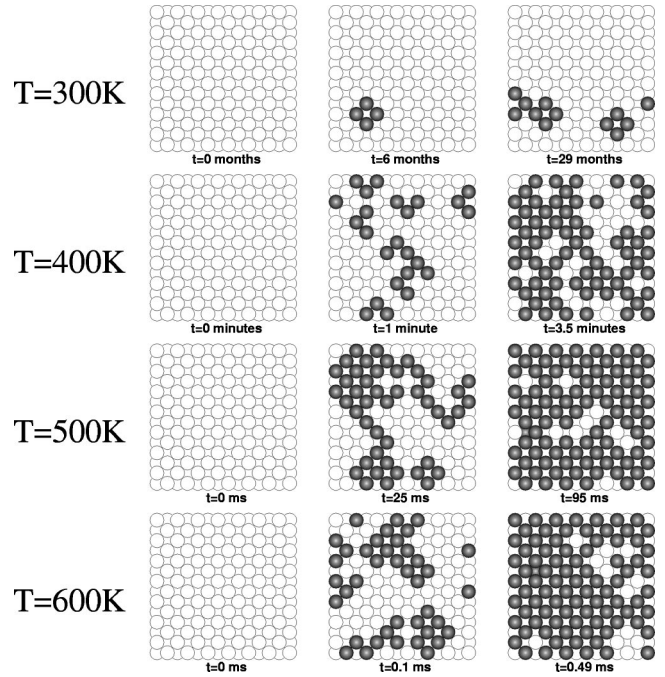


FIG. 2. Snapshots of the Ag(100) evolution at different temperatures. Atoms occupying a different position than in the initial ( $t=0$ ) state are shaded.

we used standard TAD [Eq. (3)] to simulate the exit from those states. Using  $E_{\min}=1.3 \text{ eV}$  for the flat-surface state had a huge influence on the speed of the TAD simulations: we obtained an additional boost (multiplying the one given by the standard TAD method) ranging from  $\sim 50$  (for a total boost of  $\sim 1.8 \times 10^4$  with respect to standard MD) at 600 K, to three orders of magnitude at 300 K (total boost with respect to MD:  $\sim 10^{15}$ ), making it possible to collect the results presented here in approximately two weeks of CPU time (for each  $T$ ) on one SGI R10000 workstation.

We emphasize that in this procedure the value  $E_{\min}=1.3 \text{ eV}$  for the flat-surface state was not determined by running until  $\tau$  exceeded  $\tau_{\min}$  in Eq. (5); rather,  $E_{\min}$  was simply found in a quick preliminary study. However, during the whole set of TAD simulations presented in this work, we never observed an event attempted from the flat-surface state with a barrier lower than this  $E_{\min}$ , and at the end of the simulations the total time accumulated in the state exceeded  $\tau_{\min}$  [see Eq. (5)]. Thus, after the fact, we could conclude that our estimate of  $E_{\min}$  was correct, validating all the simulations. This “gambling” approach can be very powerful, if the gamble pays off. In this case it did pay off, but if a barrier lower than the previously estimated  $E_{\min}$  had shown up during the simulations, all the simulations would have had to be restarted using the lower  $E_{\min}$ .

### C. Surface evolution

Snapshots of the surface evolution are displayed in Fig. 2, where an atom is shaded if it occupies a different position than in the initial configuration. The surface always looks flat, but, between snapshots, atoms clearly diffused within



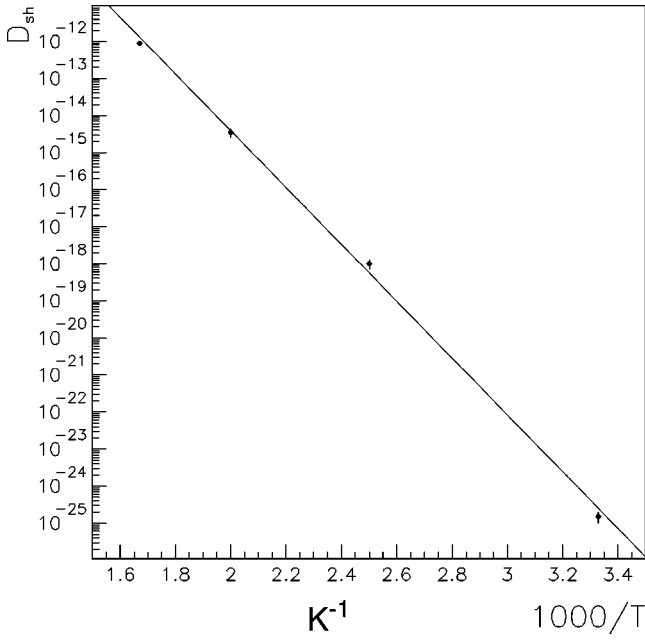


FIG. 3. Arrhenius plot representation of the tracer diffusion coefficient for a single surface atom.  $T$  is in K and  $D_{sh}$  is in  $\text{cm}^2 \text{s}^{-1}$ . The line is the best fit with  $E_{sh} = 1.52 \text{ eV}$  and  $D_0 = 8 \text{ cm}^2 \text{s}^{-1}$ .

the surface. To quantify the importance of such atomic *shuffle*, we computed the tracer diffusion coefficient  $D_{sh}$  for a surface atom at different temperatures. To this goal, we used the efficient memory expansion method of Ref. 17. An Arrhenius plot of  $\log(D_{sh})$  as a function of  $1/T$  is displayed in Fig. 3. Note that the simple law  $D_{sh} = D_0 \exp(-E_{sh}/k_B T)$  fits the data fairly well, for  $E_{sh} \sim 1.52 \text{ eV}$ , and  $D_0 \sim 8 \text{ cm}^2 \text{s}^{-1}$ .

Typical diffusion paths responsible for the surface-atom motion are shown in Fig. 4. The easiest event leading to shuffle is triggered by the formation of a simple (adatom and vacancy are adjacent) Frenkel pair (top panel of Fig. 4). After the Frenkel pair is formed [ $A \rightarrow B$ , with activation energy  $E_{AB} \sim 1.30 \text{ eV}$ ], the easiest event is the reabsorption of the pair into the surface ( $B \rightarrow A$ ,  $E_{BA} \sim 0.27 \text{ eV}$ ). If this happens, the atoms return to their initial configuration (A), and no atomic shuffle occurs. If, instead, a higher barrier is surmounted ( $B \rightarrow C$ ,  $E_{BC} \sim 0.50 \text{ eV}$ ), several atoms can easily change their position within the surface, before the adatom and the vacancy annihilate. In the figure, we have illustrated only the simple case  $B \rightarrow C$ ,  $C \rightarrow D$  ( $E_{CD} \sim 0.50 \text{ eV}$ ),  $D \rightarrow E$  ( $E_{DE} \sim 0.27 \text{ eV}$ ), but many more alternative paths are possible from configuration B, all characterized by an effective barrier  $E^{\text{FS}} \equiv E_{AB} + (E_{BC} - E_{BA}) \sim 1.53 \text{ eV}$ , where the superscript FS stands for Frenkel-pair induced shuffle. Many of these paths can lead to multiple-atom rearrangement and to large displacements. For example, if from configuration C the vacancy makes another jump so that the adatom-vacancy distance grows, a long random walk involving many atoms moves might be needed before the vacancy is annihilated. Surface shuffle is not induced by FS mechanisms only. An important alternative is displayed in the central panel of Fig. 4: three atoms are involved, one of them is pushed over the surface, and at the end the adatom (atom 3 in the figure) is not adjacent to the vacancy (V). We call this event the

knight mechanism, because of the close resemblance with the knight mechanism found by Cohen on fcc(100) surfaces.<sup>18</sup> The increased distance between the adatom and the vacancy causes an important difference from the simple Frenkel-pair formation. In this case,  $E_{AB} \sim 1.48 \text{ eV}$ ,  $E_{BC} = 0.50 \text{ eV}$ , and  $E_{BA} = 0.43 \text{ eV}$ , so that the immediate annihilation of the adatom-vacancy pair is favored by only  $0.07 \text{ eV}$ . If the vacancy jumps one site further away from the atom, the probability for the system to return to the flat-surface state without shuffling atoms is very low. As in the FS case, in the figure we only reported a simple example of a path leading to shuffle and generated by a knight mechanism. We shall call KS (knight-induced shuffle) mechanisms the set of all possible shuffle processes initiated by a knight mechanism, and with an effective activation barrier  $E^{\text{KS}} \equiv E_{AB} + (E_{BC} - E_{BA}) \sim 1.55 \text{ eV}$ . In the bottom panel of Fig. 4 another mechanism leading to a change in the positions of the surface atoms is displayed. In this case the shuffle is directly caused by a single mechanism with no vacancy: four atoms within the surface are involved, and they switch position surmounting a single saddle point. We shall call this mechanism rotation-induced shuffle (RS). We find  $E^{\text{RS}} \sim 1.54 \text{ eV}$ .

Summarizing, there are three different mechanisms whose activation energy is very close to the value  $E_{sh} = 1.52 \text{ eV}$  extracted from the Arrhenius analysis of the diffusion coefficient. Note that in the RS mechanism the number of atoms involved (4) is fixed, and they are all displaced by a single lattice site. On the other hand, paths leading to larger displacements and/or several-atom rearrangements are likely for the FS and KS mechanisms. For this reason, FS and KS give a much larger contribution (in terms of a larger prefactor) to  $D_{sh}$ .

We note that concerted events somewhat similar to those reported in this section have been found also on stepped metal surfaces.<sup>19</sup> In this subsection we described the most frequent events leading to shuffle of the surface layer. Very rarely, and only at the two highest temperatures, we also detected events causing a change in the positions of atoms occupying subsurface layers. Indeed, a careful inspection of the right panel of Fig. 2 reveals a single shaded atom (indicating that the atom has moved) in the second layer at both  $T = 500 \text{ K}$  and  $T = 600 \text{ K}$ .

#### D. Inadequacy of standard molecular dynamics

Due to the high activation energies involved, and to the relatively low temperatures considered, a standard MD simulation, run for, say, several ns, would have revealed the picture of a static surface, where all the atoms simply vibrate around their equilibrium positions. Contrasting with the shuffle behavior discussed above, we see that this picture is accurate only in the short time scale reachable with MD. In order to observe some atomic motion using standard MD, it is necessary to simulate at a very high temperature. The results obtained by simply increasing the temperature, however, would be representative of the high-temperature behavior only. This can be easily demonstrated for the system considered in this paper. We ran standard MD at  $T = 1000 \text{ K}$  (keeping the same system size used in the TAD

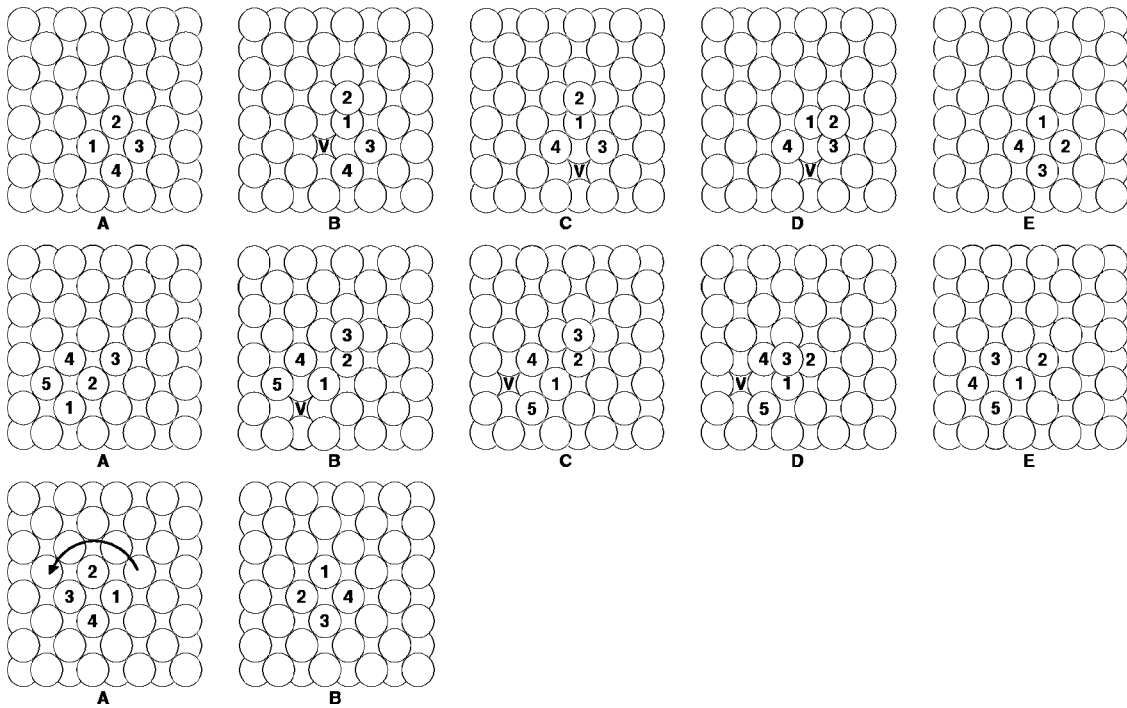


FIG. 4. Top panel: Frenkel-pair formation and one possible FS path leading to shuffle. From A to B: atom number 2 is pushed over the surface by atom 1. The process causes the formation of a vacancy (V). If (from B to C) the vacancy makes a jump, an easy way for atom 2 to annihilate the vacancy involves a single jump (from C to D), and the subsequent move leading to E. From A to E, 4 atoms change position within the surface. Central panel: knight mechanism and one possible KS path leading to shuffle. From A to B: atom number 3 is pushed over the surface by a concerted mechanism involving atoms 1 and 2, causing the formation of a vacancy V. If the vacancy moves to the position represented in C, atom 3 makes a single jump (D) and then annihilates the vacancy in (E); 5 atoms are shuffled by the mechanism. Note that passing from A to E, atom 3 makes an effective double move. Bottom panel: four-atom rotation mechanism. From A to B, 4 atoms are involved in a concerted 90° rotation. The RS mechanism directly causes shuffle of the four atoms. Note that the atom reordering (if the direction is reversed) is indistinguishable from the FS example given in the top panel.

simulations), until we reached a simulation time of 6 ns. Due to the high temperature, many mechanisms were detected, in spite of the extremely short time scale. We observed a behavior totally different from the one found at the lower temperatures in our TAD simulations. In the left panel of Fig. 5, the number  $N_{out}$  of atoms found out of the surface layer (i.e., promoted to the adlayer) is plotted as a function of  $t$ . Whereas in the TAD simulations (which were carried out in the temperature range 300–600 K) the system was observed to spend only a negligible fraction of time out of the flat-surface configuration, at  $T=1000$  K at least one atom is out of the surface layer about a third of the time. Moreover, at  $T=1000$  K, configurations where  $N_{out}>1$  are easily found. An example of the case  $N_{out}=4$  is illustrated in the right panel of Fig. 5: a cluster of four atoms is formed, leaving four vacancies in the surface layer. In contrast, our TAD simulations revealed that in the temperature range 300–600 K it is extremely unusual to have more than a single atom out of the surface layer. (At  $T=600$  K we detected a single transition causing the formation of a dimer on the surface; in all the other cases only single atoms were found). In conclusion, the dynamical evolution in a standard MD simulation on a short time scale, at either low temperature or high temperature, is not representative of the true long time-scale dynamics at the low temperature. TAD allows us to capture the

real complexity of the system dynamics on relevant time scales at the desired temperature.

**E. Spontaneous shuffle vs thermal-vacancy induced motion**

An important point to be addressed is how strongly these spontaneous shuffle processes contribute to the mobility of the surface atoms in the presence of an equilibrium concentration of surface vacancies. We recall that equilibrium-

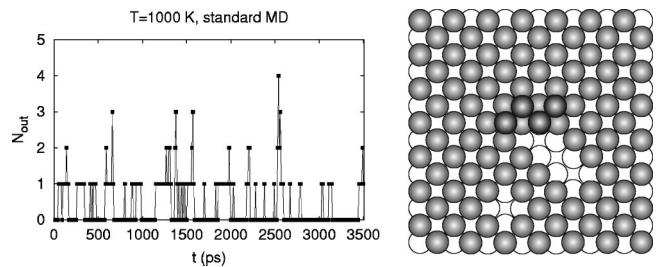


FIG. 5. Ag(100): results of a standard MD simulation at  $T=1000$  K. Left panel: number of atoms  $N_{out}$  found out of the surface layer at the time  $t$ . Right panel: configuration with  $N_{out}=4$  detected in the MD simulations. Full circles represent the four atoms laying over the surface, gray circles the surface layer, and empty circles the second layer.

vacancy induced motion (EVIM) was investigated in Refs. 2,3. If a vacancy is already present on the surface, each time it moves it induces a single-atom move within the surface. If  $E_v^f$  is the vacancy formation energy and  $E_v$  is the vacancy diffusion barrier, the effective activation energy for such a process is given by  $Q = E_v^f + E_v$ . For the system considered here, our potential gives  $Q \sim 1$  eV, so that  $Q < E_{sh}$ , meaning that at, low  $T$ , EVIM will dominate with respect to the spontaneous-shuffle induced motion (SSIM) found in this work. Still, it is conceptually important to understand that even in the absence of a thermal concentration of vacancies, atoms within a flat surface do move. For instance, let us consider a terrace on a surface, at a temperature where the equilibrium concentration of vacancies is such that there is a very small, and fluctuating, number ( $n$ ) of vacancies in the terrace. If atomic diffusion occurred purely due to EVIM, hypothetical real-time measures of the tracer diffusion coefficient  $D_T$  for the terrace atoms would yield a certain value of  $D_T$  for each value of  $n$ , and zero when  $n=0$ . Instead, SSIM guarantees that  $D_T > 0$  at all times. Moreover, one could imagine realistic out-of-equilibrium situations where the thermal concentration of vacancies is lowered (e.g., during growth), so that the relative importance of the spontaneous shuffle is enhanced.

We wish to stress that a simple comparison between  $Q$  and  $E_{sh}$  is not enough to reveal the relative importance of shuffle and equilibrium-vacancy induced motion. As we pointed out above,  $D_{sh}$  is characterized by a very large prefactor, due to the nature of the FS and KS mechanisms. As a consequence, we expect SSIM to become more important with respect to EVIM as  $T$  is increased. In the whole range considered here, EVIM still dominates, although SSIM may dominate for other materials.

Finally, we note that the values of  $D_{sh}$  at 500 and 600 K that we extracted from the Arrhenius plot of Fig. 3 might underestimate the real ones, because of finite-size effects. Indeed, at the two highest temperatures, we occasionally observed the vacancy and/or the adatom moving so far one from the other that the annihilation was forced by the imposed periodic boundary conditions. By significantly increasing the simulation cell size (which we could not afford to do), the effective displacements caused by these events would have been larger.

### F. Anharmonic effects

If the rate of every possible diffusion mechanism is given by Eq. (1), TAD describes the exact dynamics of the system (with confidence  $1 - \delta$ ). However, deviation from the Arrhenius behavior can occur, especially at high temperatures. As explained in Sec. II A, in the TAD method the escape times from a given state at a temperature  $T_{low}$  are extrapolated from the corresponding times at  $T_{high} > T_{low}$ . If anharmonic effects are present at  $T_{high}$ , the extrapolation procedure will transfer them to  $T_{low}$  as well. If  $T_{low}$  is particularly low, anharmonic effects are not expected, so that the rates extrapolated to  $T_{low}$  from the ones at  $T_{high}$  will suffer from an extrapolation error.<sup>5</sup> A possible way to check for

anharmonicity errors, for a mechanism with activation energy  $E$ , is to determine its real rate  $k_{real}$  at  $T_{high}$ , as extracted from MD simulations, and compare it with the hTST rate  $k_{hTST}$  given by Eq. (1). The necessary frequency prefactor  $\nu_{0,i}$  can be computed using the Vineyard expression<sup>12</sup>

$$k_{hTST} = \frac{\prod_i^{3N} \nu_i^m}{\prod_i \nu_i^s} \exp(-E/k_B T_{high}), \quad (6)$$

where  $N$  is the number of moving atoms in the system,  $\nu_i^m$  represents the  $i$ th normal mode at the minimum, and  $\nu_i^s$  the  $i$ th normal mode at the saddle. To boost the dynamics out of the flat-surface state, we had to use a very high value for  $T_{high}$  (1000 K; see Sec. III A), because of the extremely high activation energies for every possible mechanism taking the system out of this state. As a consequence, some anharmonicity in the rate can be expected. We looked for anharmonic effects for the Frenkel-pair formation mechanism. At  $T_{high} = 1000$  K, the ratio  $\gamma_{1000}$  defined by  $\gamma_{1000} \equiv k_{real}/k_{hTST}$  is  $\sim 3$ . However, this does not automatically mean that the corresponding extrapolated rates at  $T_{low}$  are affected by an error of a factor 3. If  $\gamma_{T_{high}} = \gamma_{T_{low}}$ , then the extrapolation procedure [Eq. (2)] is still exact. For example, we found  $\gamma_{800} \sim \gamma_{1000}$ , so that a TAD simulation run with  $T_{high} = 1000$  K and  $T_{low} = 800$  K would have generated the correct rate for the Frenkel-pair formation at  $T_{low} = 800$  K, in spite of the fact that the rates are anharmonic. (It was not possible to collect enough events to compute a statistically meaningful  $\gamma_T$  for  $T < 800$  K.) On the other hand, we know that  $\gamma_T \rightarrow 1$  for  $T \rightarrow 0$ , so that for a sufficiently low  $T_{low}$ , the extrapolated rates will be 3 times larger than the real ones. In conclusion, at the  $T_{low}$  values considered in our simulations, the Frenkel-pair formation rates were artificially enhanced by a factor between 1 and 3. At  $T = 300$  K the error was probably close to the full factor of 3. We realize that for some systems, such an error can be considered unacceptable. In this case, though, we note that a simple  $\sim 5\%$  rescaling of the mechanism barrier would induce such a difference in the rates, so this anharmonicity error is probably smaller than the error typically accepted as unavoidable when using semi-empirical potentials. Anharmonic errors can be lowered by using a lower  $T_{high}$ . For example, we checked the anharmonic errors for a randomly chosen set of mechanisms found in the growth simulations of Ref. 13, where we used  $T_{high} \leq 600$  K. The anharmonic error was always less than a factor of 2.

## IV. CONCLUSIONS

In this paper we investigated, by TAD simulations, the evolution of an ideal Ag(100) surface well below its melting point. Exploiting the enhanced boost in the dynamics offered by the most recent version of TAD,<sup>6</sup> we were able to reach extremely long time scales, and to detect important diffusion mechanisms involving the surface atoms. In particular, we

showed that, with no preexisting vacancies, atoms are shuffled by complex events, which in most cases involve the formation of short-lived adatom–vacancy pairs.

In a recent study demonstrating the importance of surface vacancies in surface diffusion, the authors of Ref. 2 cleverly titled their paper “Nothing moves a surface.” Perhaps we have shown here that *everything* moves a surface.

## ACKNOWLEDGMENTS

We acknowledge fruitful discussions with B.P. Uberuaga. This work was supported by the United States Department of Energy, Office of Basic Energy Sciences, under DOE Contract No. W-7405-ENG-36 and by the Italian MURST, under Project No. 9902112831.

\*E-mail address: Francesco.Montalenti@unimib.it

- <sup>1</sup>P.J. Feibelman, Phys. Rev. Lett. **65**, 729 (1990); Z.-P. Shi, Z. Zhang, A.K. Swan, and J.F. Wendelken, *ibid.* **76**, 4927 (1996); P. Salo, J. Hirvonen, I.T. Koponen, O.S. Trushin, J. Heinonen, and T. Ala-Nissila, Phys. Rev. B **64**, 161405(R) (2001); T.R. Linderoth, S. Horch, L. Petersen, S. Helveg, E. Laegsgaard, I. Stensgaard, and F. Besenbacher, Phys. Rev. Lett. **82**, 1494 (1999); F. Montalenti and R. Ferrando, *ibid.* **82**, 1498 (1999); T. Ala-Nissila, R. Ferrando, and S.C. Ying, Adv. Phys. **51**, 949 (2002).
- <sup>2</sup>R. van Gastel, E. Somfai, S.B. van Albada, V. van Saarloos, and J.W.M. Frenken, Phys. Rev. Lett. **86**, 1562 (2001).
- <sup>3</sup>M.L. Grant, B.S. Swartzentruber, N.C. Bartelt, and J.B. Hannon, Phys. Rev. Lett. **86**, 4588 (2001).
- <sup>4</sup>K.F. McCarty, J.A. Nobel, and N.C. Bartelt, Nature (London) **412**, 622 (2001).
- <sup>5</sup>M.R. Sørensen and A.F. Voter, J. Chem. Phys. **112**, 9599 (2000).
- <sup>6</sup>F. Montalenti and A.F. Voter, J. Chem. Phys. **116**, 4819 (2002).
- <sup>7</sup>A.F. Voter, F. Montalenti, and T.C. Germann, Annu. Rev. Mater. Res. **32**, 321 (2002).
- <sup>8</sup>M.S. Daw and M.I. Baskes, Phys. Rev. B **29**, 6443 (1984).
- <sup>9</sup>A.F. Voter in *Modeling of Optical Thin Films*, edited by M.R. Jacobson, Proc. SPIE **821**, 214 (1987); A.F. Voter (unpublished).
- <sup>10</sup>B.D. Yu and M. Scheffler, Phys. Rev. B **56**, 15 569 (1997).
- <sup>11</sup>M.H. Langelaar, M. Breeman, and D.O. Boerma, Surf. Sci. **352-354**, 597 (1996).
- <sup>12</sup>G.H. Vineyard, J. Phys. Chem. Solids **3**, 121 (1957).
- <sup>13</sup>F. Montalenti, M.R. Sørensen, and A.F. Voter, Phys. Rev. Lett. **87**, 126101 (2001).
- <sup>14</sup>K.D. Stock and E. Menzel, J. Cryst. Growth **43**, 135 (1978); H. Häkkinen and M. Manninen, Phys. Rev. B **46**, 1725 (1992).
- <sup>15</sup>G. Henkelman, B.P. Uberuaga, and H. Jónsson, J. Chem. Phys. **113**, 9901 (2000); G. Henkelman and H. Jónsson, *ibid.* **113**, 9978 (2000).
- <sup>16</sup>The activation energies change slightly at different temperatures due to thermal expansion. For example, the barrier for the Frenkel-pair formation is 1.30, 1.29, 1.28, 1.28, and 1.27 eV at the 0, 300, 400, 500, and 600 K lattice parameters, respectively. In the text we report values corresponding to  $T=0$  K, while the correct value for each temperature was employed as  $E_{\min}$ .
- <sup>17</sup>S.C. Ying, I. Vattulainen, J. Merikoski, T. Hjelt, and T. Ala-Nissila, Phys. Rev. B **58**, 2170 (1998).
- <sup>18</sup>J.M. Cohen, Surf. Sci. **306**, L545 (1994).
- <sup>19</sup>J. Merikoski and T. Ala-Nissila, Phys. Rev. B **52**, R8715 (1995).